J. CHEM. SOC. FARADAY TRANS., 1990, 86(1), 11-16 11

# Translational Energy Dependence of Reaction Dynamics in Kinematically Constrained Systems

## Xe($^3P_2$) + HCl, HBr, HI and CH$_3$I

**William S. Hartree† and John P. Simons**
*Chemistry Department, The University, Nottingham NG7 2RD*

---

The fully dispersed chemiluminescence spectra excited by reactions of Xe($^3P_2$) with HI, HBr, HCl and CH$_3$I have been recorded under superthermal beam–Maxwellian gas conditions. Direct spectral inversion has enabled determination of the rare-gas halide product vibrational energy distributions at selected collision energies in the range $\langle E_T \rangle \approx$ (4–90)kJ mol$^{-1}$. The mean vibrational energy disposals $\langle E'_v \rangle$ are found to increase linearly with the mean collision energy $\langle E_T \rangle$. This result, together with earlier measurements of reactive excitation functions (K. M. Johnson, J. P. Simons, P. A. Smith, C. Washington and A. Kvaran, *Mol. Phys.*, 1986, **57**, 255) and with the kinematic constraint on the dynamics, allows separate estimates of the mean energy disposals into rotation and translation, as well as the mean reactive cross-section.

---

In reactive collisions of the type

$$A + BC \rightarrow (AB)_{v'j'} + C \qquad (1)$$

where the mass of the fragment C is much less than that of A or B, angular momentum conservation necessarily channels reagent orbital angular momentum $\boldsymbol{L}$ into product internal rotation $\boldsymbol{J}'$.[1] In the classical, kinematic limit, where $|\boldsymbol{L}| \gg |\boldsymbol{J}|$ and $|\boldsymbol{L}'| \ll |\boldsymbol{J}'|$, the equality

$$|\boldsymbol{L}| \equiv |\mu \boldsymbol{v}_{\rm rel} b| \approx |\boldsymbol{J}'| \qquad (2)$$

provides a link between vibrationally resolved, product rotational state distributions and the distribution of reactive impact parameters, $b$;[2] ($\mu$ is the reagents' reduced mass, $\boldsymbol{v}_{\rm rel}$ their relative velocity). The validity of eqn (2) has been tested through measurement of product rotational alignment, $\langle P_2(\hat{\boldsymbol{v}}_{\rm rel} \cdot \hat{\boldsymbol{J}}') \rangle$, in reactions of alkali-metal atoms[3–5] or their analogues, metastable electronically excited heavy rare-gas atoms[6–8] [*e.g.* Xe*(5$p^5$6s)], with hydrogen halides and with methyl iodide.[5,8,9] Alignment studies have established the attainment of the kinematic limit at superthermal collision energies[6] for the reactions

$$\text{Xe}(^3\text{P}_2) + \text{HX} \rightarrow \text{XeX}^*(\text{B, C}) + \text{H}; \quad \text{X} \equiv \text{Cl, Br, I} \qquad (3)$$

but not for the reaction[8]

$$\text{Xe}(^3\text{P}_2) + \text{CH}_3\text{I} \rightarrow \text{XeI}^*(\text{B, C}) + \text{CH}_3. \qquad (4)$$

At near-thermal collision energies, where rotational alignment of the rare-gas halides produced in reaction (3) falls away from its limiting value, $\langle P_2(\hat{\boldsymbol{v}}_{\rm rel} \cdot \hat{\boldsymbol{J}}') \rangle = -\frac{1}{2}$, the inequality $|\boldsymbol{L}'| \ll |\boldsymbol{J}'|$ is less pronounced.[6,7]

Noda and Zare[10] have developed a simple dynamical model for kinematically constrained reactions in which the product recoil energy is taken to be a constant, the CPR model. This rests on the assumption of collisions proceeding *via* the same critical configuration regardless of the initial collision conditions, when the departing atom is light and mobile. Imposition of this additional constraint leads to both rotational *and* vibrational product energy distributions being subject to kinematic control. The model predicts vibrational energy distributions which are typically bell-shaped, with widths that increase with the collision energy, but which peak at a constant vibrational energy determined simply by the difference between the reaction exoergicity and reagent internal energy, ($\Delta E_0 + E_{\rm int}$), and the recoil energy, $E'_{\rm T}$. Classical trajectory calculations by Siegel and Schultz[11] gave support to the CPR assumption, at least for certain kinds of potential-energy surface, but there have been very few experimental tests beyond the examples of Ba reacting with HX (X ≡ F, Cl, Br, I)[2,12,13] or CH$_3$Br.[14] Such experiments are themselves constrained, either by the severe structural congestion in the LIF spectra of the heavy alkaline-earth-metal halides or the absence of suitable LIF transitions in the alkali-metal halides.[15] In the present work, these problems have been by-passed by studying the spontaneously chemiluminescent reactions (3). The collisional energy dependence of the vibrational energy disposal in the newly formed rare-gas halides, XeX(B, C) (X ≡ Cl, Br, I), has been explored through analysis of their dispersed chemiluminescence spectra recorded under superthermal atomic beam–Maxwellian gas conditions. The pulsed atomic beam, generated *via* 'tunable' rotor acceleration, allows measurements of the chemiluminescent reaction channels over the collision energy range $\langle E_T \rangle \approx$ (4–90) kJ mol$^{-1}$.[6]

The patterns of energy disposal among the reaction products, which are discussed in the light of the CPR assumption, contrast strongly with those found in the corresponding Ba/HX systems,[12,13,16,17] but not with the (limited) data available for the more closely analogous alkali-metal/HX reactions.[17] New data for the system Xe($^3$P$_2$)/CH$_3$I also run closely parallel to those for the corresponding alkali-metal atomic reactions.[17]

## Experimental

Dispersed chemiluminescence emission spectra were recorded under effusive, and under superthermal beam-gas conditions. The rotor-accelerated, metastable atomic beam source and the computer-controlled data acquisition system have been described elsewhere.[18–21] In the present experiments, an atomic beam of Xe($^3$P$_2$) was directed into a differentially pumped fluorescent cell, through which the target gas was flowed, typically at pressures 1.6–3.3 Pa, to excite chemiluminescent emission from XeI, XeBr or XeCl (B, C) under single-collision conditions. The spectra dispersed on a grating monochromator, were recorded using gated photon-counting techniques, at a band-pass, typically set to 1.3 nm. The UV detection sensitivity was calibrated absolutely, against a standard deuterium lamp.

---

† Present address: School of Chemistry, The University, Bristol BS8 1TS.

### Spectral Inversion

The nascent vibrational population distributions in the rare-gas halides produced through reactions (3) or (4) were obtained through direct inversion of the oscillatory fluorescence continua associated with the XeX(B → X) transitions. Full details of the method have been described elsewhere:[22,23] a small modification was included in the present work to accommodate the wavelength dependence of the monochromator response function, assumed to be triangular.[24] Optimised parameters for the XeX, B($\frac{1}{2}$) and X($\frac{1}{2}$) potentials were taken from the data listed by Johnson *et al.*,[6,22,23] Hay and Dunning[25] and Tamagake *et al.*[26]

## Results

Chemiluminescence spectra, excited through the beam-gas reaction of Xe($^3P_2$) with HI at both thermal and superthermal average collision energies, $\langle E_T \rangle$ are shown in fig. 1. The spectrum at thermal energy, $\langle E_T \rangle = 3.9$ kJ mol$^{-1}$, is in good agreement with that recorded earlier under discharge flow or bulk gas conditions.[6] Each of the spectra comprise three distinct bound → free continua B($\frac{1}{2}$) → X($\frac{1}{2}$), C($\frac{3}{2}$) → A($\frac{3}{2}$) and B($\frac{1}{2}$) → A($\frac{1}{2}$) which, at thermal collision energy, are easily separated. As the collision energy is increased, however, they begin to overlap because of increasing intensity in the short-wavelength tails. The shift in the short-wavelength limit of the B → X component is particularly clear in the sequence of chemiluminescence spectra recorded at higher resolution and shown in fig. 2(*a*). The shifts reflect the contribution from increasingly highly excited vibrational states in the reaction products generated at elevated collision energies. Similar behaviour is displayed in the Xe($^3P_2$)/HBr raction system, see fig. 2(*b*). On the other hand, there is no significant change in the *relative* contributions made by fluorescence from the closely lying B($\frac{1}{2}$) and C($\frac{3}{2}$) states: the ratio of the integrated areas under the B → X and C → A bands in XeI remains near constant at a value (2.5–2.6). Fig. 2(*c*) shows the chemiluminescence emission from XeCl(B → X), excited *via* the endothermic reaction of Xe($^3P_2$) with HCl, at a collision energy of 40.6 kJ mol$^{-1}$.

XeI(B → X) spectra excited by collisions of Xe($^3P_2$) with $CH_3I$ are shown in fig. 3. The chemiluminescent reaction has a very low branching ratio,[8] so the spectra are relatively noisy but despite this, the similarity between the spectral contours recorded at thermal energy and at high collision energies suggests little change in the average energy disposal in vibrational excitation, a result in marked contrast with the behaviour found for the hydrogen halides.

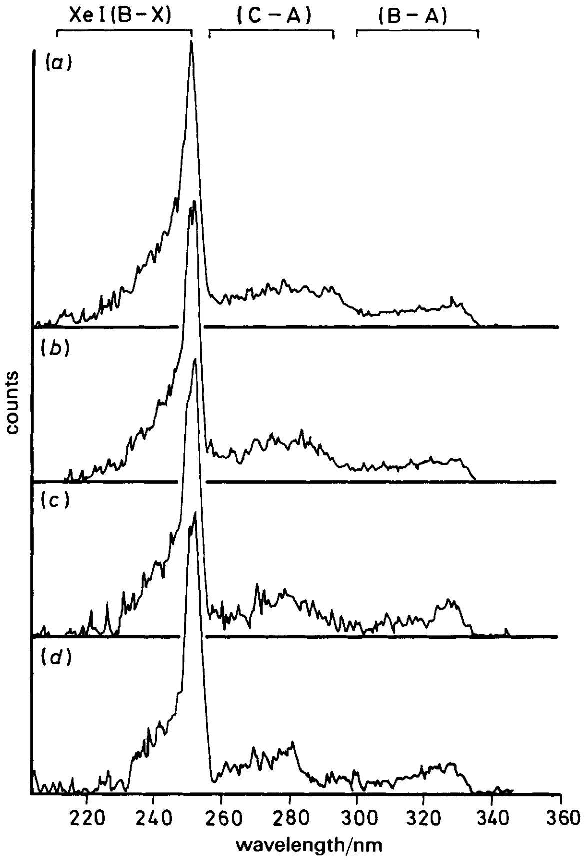

**Fig. 1.** Chemiluminescence excited by collisions of Xe($^3P_2$) with HI. Monochromator band pass, 2 nm. Mean collision energy, $\langle E_T \rangle$/kJ mol$^{-1}$: (*a*) 65.2, (*b*) 43.4, (*c*) 31.2, (*d*) 3.8.

### Vibrational Population Distributions

Spectral inversion of the B → X chemiluminescence continua leads to the nascent vibrational population histograms shown in fig. 4 (calculated from the observed steady-state distributions by weighting with the appropriate Einstein coefficients[6]). The distributions confirm the qualitative conclusions drawn above: namely the population of increasingly high vibrational levels with increasing collision energy in the reaction with HI, HBr (and HCl). In each case the spectral inversion leads to distributions in which all levels are populated up to the limit imposed by energy conservation. (It should be emphasised that no energy-conservation constraints were introduced into the inversion procedure to limit the population spread.)

In the Xe($^3P_2$)/$CH_3I$ system, the low chemiluminescence yields reduced the precision of the spectral inversion and the data at thermal collision energy could not be quantitatively analysed. At the higher collision energies, however, it was possible to confirm the relative *in*sensitivity of the vibrational energy disposal to increasing collision energy, and in particular the absence of populations in the more highly excited, energetically accessible vibrational levels. For example, at a mean collision energy $\langle E_T \rangle = 31.2$ kJ mol$^{-1}$, the highest accessible level $v_{XeI(B)} > 120$, but the highest populated level lies at $V_{XeI(B)} \approx 40$, only.

In the discussion which follows, the vibrational population distributions are assumed to be unaffected by intersystem crossing between near-degenerate vibrational levels in the neighbouring B($\frac{1}{2}$) and C($\frac{3}{2}$) states, prior to their subsequent radiative decay. The assumption is based upon the constancy of the B → X and C → A fluorescence intensity ratios, regardless of the changes in vibrational excitation in the fluorescent products imposed by changes in collision energy.

## Discussion

### Xe($^3P_2$)/HCl, HBr, HI

The mean vibrational energies $\langle E'_v \rangle$ disposed into the rare-gas halide products together with the fractional energy disposals $\langle f'_v \rangle \equiv \langle E'_v \rangle / (\langle E_T \rangle + \langle E_R \rangle + \Delta E_0)$ are listed in table 1, where they are compared with experimental data for some related systems, and some previous (more accurate) data recorded for thermal collision energies under discharge flow conditions.[6] In the hydrogen halide systems, Xe($^3P_2$)/HI, HBr, the vibrational energy $\langle E'_v \rangle$ is found to increase almost linearly with the mean collision energy $\langle E_T \rangle$, see fig. 5. Assuming a mean energy balance

$$\langle E_T \rangle + \langle E_R \rangle + \Delta E_0 = \langle E'_v \rangle + \langle E'_R \rangle + \langle E'_T \rangle \qquad (5)$$

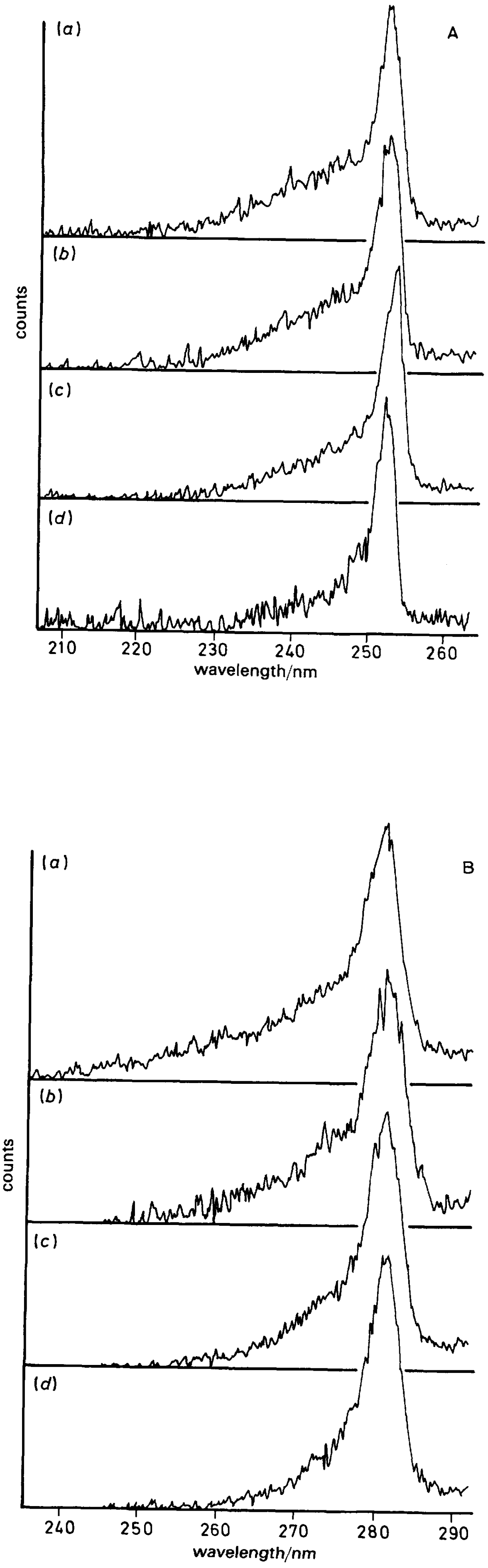

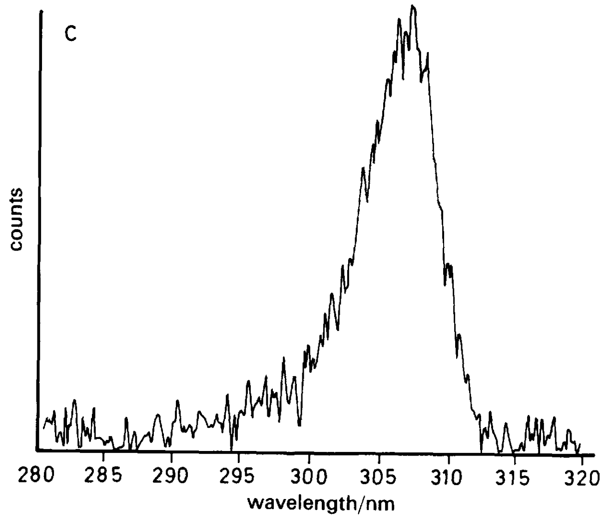

**Fig. 2.** XeX(B → X) fluorescence spectra excited by collision of Xe($^3P_2$) with (A) HI, (B) HBr, (C) HCl. $\langle E_T \rangle$/kJ mol$^{-1}$: A (*a*) 87.4, (*b*) 65.2, (*c*) 31.2, (*d*) 3.8; B (*a*) 68.8, (*b*) 51.2, (*c*) 24.9, (*d*) 3.8; C, 40.6.

where $\Delta E_0$ is the reaction exoergicity, $\langle E_R \rangle \equiv RT$ is the mean reagent rotational energy, $\langle E'_R \rangle$, $\langle E'_T \rangle$ are the mean energy disposals into rotation and translation, and taking the kinematic angular momentum constraint into account, eqn (5) can be rewritten as

$$\langle E'_v \rangle = \langle E_T \rangle [1 - \tfrac{1}{2}(b_m/r_e)^2] + [\Delta E_0 + RT - \langle E'_T \rangle]. \quad (6)$$

Here $b_m$ is the maximum reactive impact parameter, $r_e$ is the equilibrium bond length in the XeI(B) or XeBr(B) product, and the reactive opacity function (averaged over all product vibrational states), is taken to be a step function

$$P(b, E_T) = \text{a constant}; \quad 0 \leqslant b \leqslant b_m \qquad (7)$$
$$= 0; \quad b > b_m$$

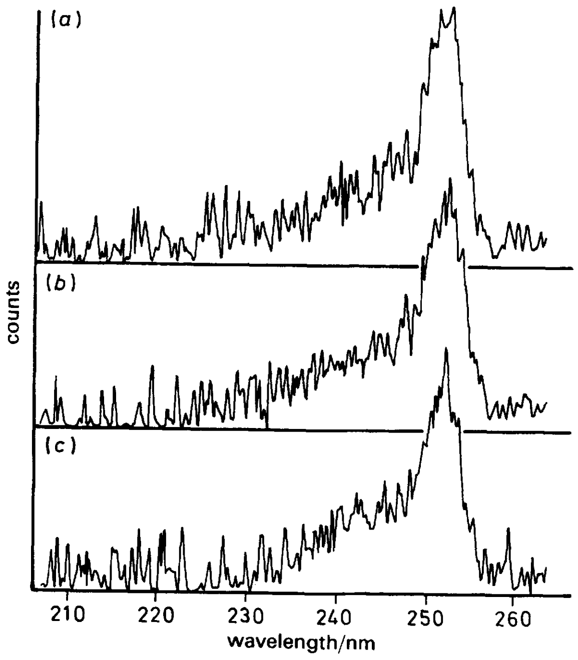

**Fig. 3.** XeI(B → X) fluorescence excited in collisions of Xe($^3P_2$) with $CH_3I$. Monochromator band-pass, 1.3 nm. $\langle E_T \rangle$/kJ mol$^{-1}$: (*a*) 68.5, (*b*) 32.6, (*c*) 3.9.

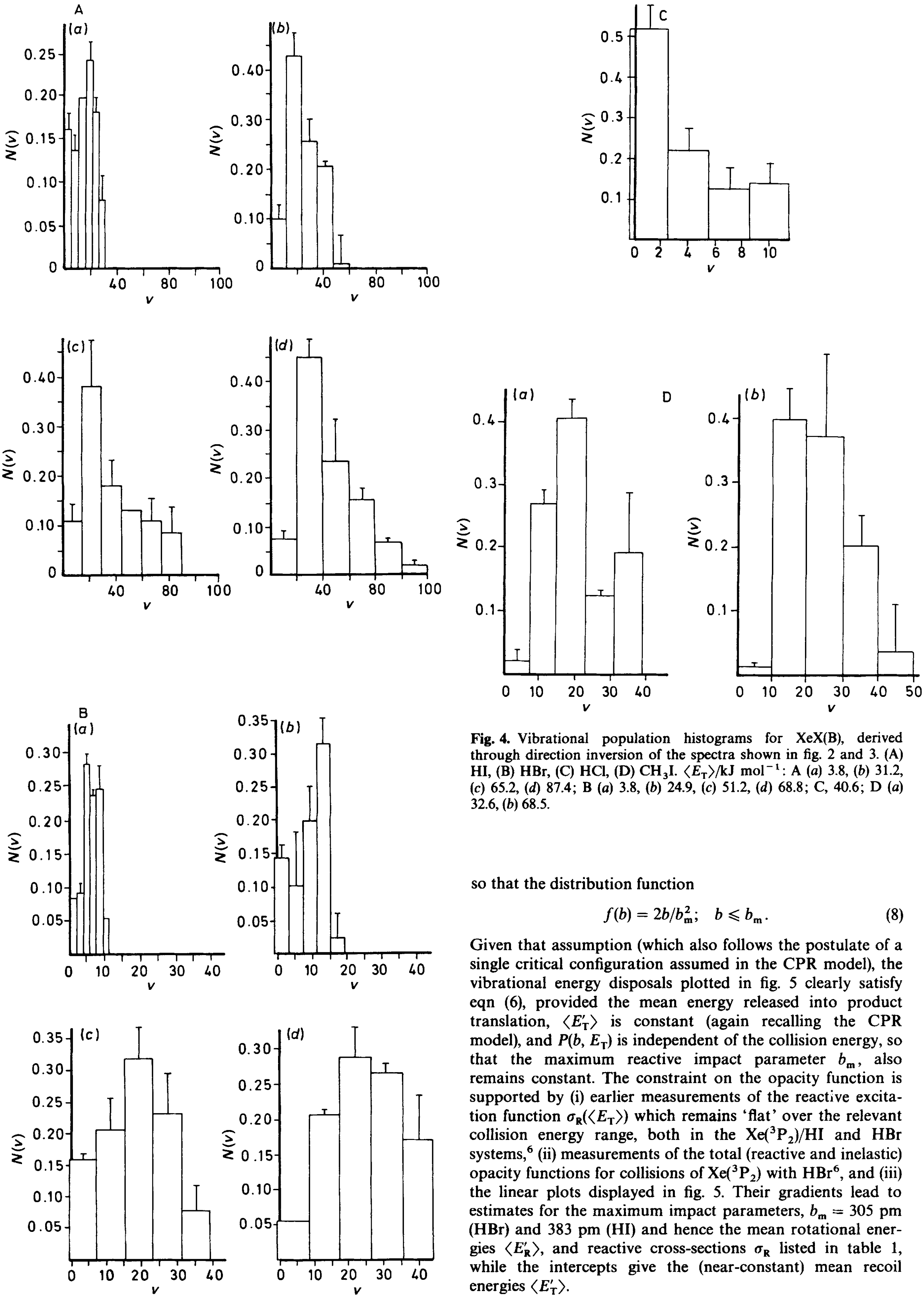

**Fig. 4.** Vibrational population histograms for XeX(B), derived through direction inversion of the spectra shown in fig. 2 and 3. (A) HI, (B) HBr, (C) HCl, (D) $CH_3I$. $\langle E_T \rangle$/kJ $mol^{-1}$: A (*a*) 3.8, (*b*) 31.2, (*c*) 65.2, (*d*) 87.4; B (*a*) 3.8, (*b*) 24.9, (*c*) 51.2, (*d*) 68.8; C, 40.6; D (*a*) 32.6, (*b*) 68.5.

so that the distribution function

$$f(b) = 2b/b_m^2; \quad b \leqslant b_m. \tag{8}$$

Given that assumption (which also follows the postulate of a single critical configuration assumed in the CPR model), the vibrational energy disposals plotted in fig. 5 clearly satisfy eqn (6), provided the mean energy released into product translation, $\langle E'_T \rangle$ is constant (again recalling the CPR model), and $P(b, E_T)$ is independent of the collision energy, so that the maximum reactive impact parameter $b_m$, also remains constant. The constraint on the opacity function is supported by (i) earlier measurements of the reactive excitation function $\sigma_R(\langle E_T \rangle)$ which remains 'flat' over the relevant collision energy range, both in the Xe($^3P_2$)/HI and HBr systems,[6] (ii) measurements of the total (reactive and inelastic) opacity functions for collisions of Xe($^3P_2$) with HBr[6], and (iii) the linear plots displayed in fig. 5. Their gradients lead to estimates for the maximum impact parameters, $b_m = 305$ pm (HBr) and 383 pm (HI) and hence the mean rotational energies $\langle E'_R \rangle$, and reactive cross-sections $\sigma_R$ listed in table 1, while the intercepts give the (near-constant) mean recoil energies $\langle E'_T \rangle$.

**Table 1.** Energy disposal data for reactions of Xe($^3P_2$) (and some representative alkali and alkaline-earth metals) with hydrogen halides and methyl iodide (mean energies are in kJ mol$^{-1}$)

| $\Delta E_0$ | $\langle E_T \rangle$ | $\langle E'_v \rangle$ | $(\langle f'_v \rangle)$ | $\sigma_R$/Å$^2$ | $\langle E'_R \rangle$ | $\langle E'_T \rangle$ | ref. |
|---|---|---|---|---|---|---|---|
| | | | Xe($^3P_2$)/HCl | | | | |
| +16 | 40.6 | 9.4 | (0.32) | — | — | — | *a* |
| | | | Xe($^3P_2$)/HBr | | | | |
| −12 | 3.8 | 9.0 | (0.50) | 38 | 2.0$^b$ | 8$^c$ | *a*, *d* |
| | 24.9 | 19.0 | (0.48) | | 13.2$^b$ | 8$^c$ | *a* |
| | 51.2 | 30.1 | (0.46) | | 27.2$^b$ | 8$^c$ | *a* |
| | 68.8 | 38.9 | (0.47) | | 36.3$^b$ | 8$^c$ | *a* |
| | | | K/HBr | | | | |
| −18 | 8.8 | *ca.* 13 | (*ca.* 0.5) | 34 | 5.5 | *ca.* 8 | *e*, *f* |
| | | | Ba/HF | | | | |
| −18 | 13.0 | 8.8 | (0.26) | — | 8.8 | 6.3 | *g* |
| | | | Xe($^3P_2$)/HI | | | | |
| −30 | 3.8 | 19.0 | (0.57) | 51 | 2.6$^b$ | 15$^c$ | *a*, *d* |
| | 31.2 | 30.0 | (0.47) | | 20.9$^b$ | 15$^c$ | *a* |
| | 65.2 | 43.0 | (0.44) | | 43.5$^b$ | 15$^c$ | *a* |
| | 87.4 | 51.0 | (0.43) | | 58.5$^b$ | 15$^c$ | *a* |
| | | | Xe($^3P_2$)/CH$_3$I | | | | |
| −91 | 3.9 | 27.6 | (0.29) | — | — | — | *h* |
| | 32.6 | 25.9 | (0.21) | | — | — | *a* |
| | 68.5 | 27.7 | (0.17) | | — | — | *a* |
| | | | Cs/CH$_3$I | | | | |
| −123 | *ca.* 7 | *ca.* 37 | (0.30) | 76 | *ca.* 5 | *ca.* 88 | *e*, *i* |

[a] Present work. [b] Calculated from estimated maximum reaction impact parameters, $b_m$. [c] Determined from data plotted in fig. 5 (see Discussion and also the following paper). [d] A. Gupta, D. S. Perry and R. N. Zare, *J. Chem. Phys.*, 1980, **72**, 6237. [e] K. Johnson, J. P. Simons, P. A. Smith, C. Washington and A. Kvaran, *Mol. Phys.*, 1986, **57**, 255. [f] C. Maltz and D. R. Herschbach, *Faraday Discuss. Chem. Soc.*, 1967, **44**, 176. [g] K. T. Gillen, C. Riley and R. B. Bernstein, *J. Chem. Phys.*, 1969, **50**, 4019. [h] D. W. Setser, T. Dreiling, H. Brashears and J. Kolts, *Faraday Discuss. Chem. Soc.*, 1979, **67**, 255. [i] See table 2.11 in B. E. Holmes and D. W. Setser, *Physical Chemistry of Fast Reactions*, ed. I. W. M. Smith (Plenum Press, New York, 1980), chap. 2

Despite the apparent constancy of the mean recoil energy, the behaviour of the vibrational population distributions is not wholly in agreement with the prediction of the CPR model. Their increasing widths with increasing collision energy might be accommodated[10] but not the accompanying shift of the peak populations $N(v_{pk})$, towards higher vibrational levels. At low collision energies, $E_T \approx 0$, the model predicts[10]

$$(v_{pk} + \tfrac{1}{2}) = (\Delta E_0 + \langle E_R \rangle - \langle E'_T \rangle)/\omega_e \qquad (9)$$

where $\omega_e$ is the product's vibrational wavenumber; the estimated values of $\langle E'_T \rangle$ lead to $v_{pk} \approx 4$ (HBr) and 13 (HI), slightly below the observed values at thermal collision energy and lying further and further below the observed values as $\langle E_T \rangle$ is increased.

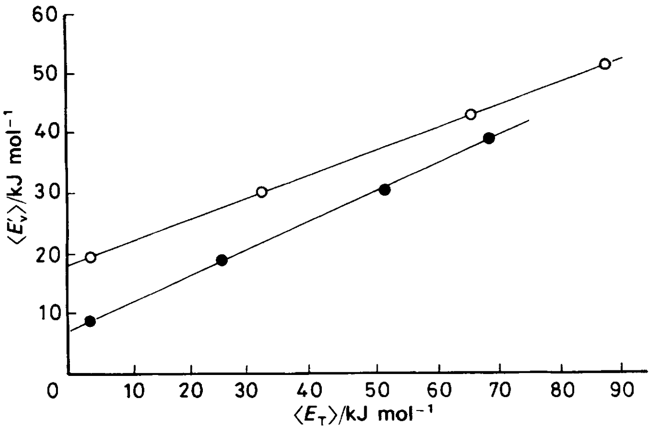

**Fig. 5.** Mean vibrational energies $\langle E'_v \rangle$ in XeBr, XeI(B) generated through reaction of thermal and superthermal atomic beams of Xe($^3P_2$) with HBr (●) and HI (○) at 300 K.

The proportionality between $\langle E_T \rangle$ and the product rotational energy $\langle E'_R \rangle$ demonstrated by the linear gradient of fig. 5 (and a necessary consequence of angular momentum conservation in the kinematic limit) has also been demonstrated by Zare and co-workers[13] and by Siegel and Schultz[12] in the kinematically analogous reactions of Ba with HF, HCl and HBr. The analogy with the metastable rare-gas reactions ends there, however, since the vibrational energy disposals in the barium halide products are far lower (see table 1) and also less sensitive to increases in the reagent collision energy. This is particularly so for the reaction of Ba with HBr and HI,[12] where Polanyi's rule[27]

$$\langle \Delta E_T \rangle \rightarrow \langle \Delta E'_T \rangle + \langle \Delta E'_R \rangle \qquad (10)$$

is well obeyed ($\langle \Delta E_T \rangle$ represents the mean reagent translational energy above any energy barrier). It clearly does not operate for the corresponding reactions of Xe($^3P_2$) where the patterns of energy disposal are much more like those of the alkali metals[17] (see table 1). Despite the strong kinematic constraints, dynamical factors associated with the nature of the reactive potential-energy surface are also of great importance. Shapiro and Zeiri,[28] who constructed a family of semi-empirical potential-energy surfaces for the alkali-metal systems, found that increasing the mass of the halogen atom promoted a reduction in the barrier height and a corresponding movement of the saddle point down into the reagent entrance valley. In the endothermic system Xe($^3P_2$)/HCl, reaction is strongly promoted by vibrational excitation of the HCl,[29] which strongly suggests a barrier in the exit valley when the halogen atom is light, while the increasing values of $\langle f'_v \rangle$ at thermal collision energies, in the sequence

HCl < HBr < HI are consistent with a similar movement of the saddle point (see table 1).

## $Xe(^3P_2)/CH_3I$

The experimental data, while of lower quality are good enough to establish the great contrast with those for $Xe(^3P_2)/HX$. The mean energies released into vibration, $\langle E'_v \rangle$, are little changed by increasing the collision energy and for *this* system, Polanyi's rule (10) *is* followed, a result which parallels the behaviour of the alkali-metal systems, K, $Rb/CH_3I$, in which the transfer $\langle \Delta E_T \rangle \rightarrow \langle \Delta E'_T \rangle$ has an efficiency of $d\langle \Delta E'_T \rangle / d\langle \Delta E_T \rangle > 0.5$.[30,31] The adherence to Polanyi's rule implies a predominance of low reactive impact parameters, leading to a high probability of 'induced repulsive energy release'.[31] Earlier measurements of the product rotational alignments reinforce this; although the average alignments increased with the collision energy, they remained well below the kinematic limit $\langle P_2(\hat{J}' \cdot \hat{v}_{rel}) \rangle = -0.5$ and also well below the limiting, high-energy value, $-0.45$, calculated[21] *via* the DIPR-DIP[32–34] model.

This is not too surprising since the assumptions of the DIPR model, while appropriate for the conversion of reaction exothermicity into product repulsion, $\Delta E_0 \rightarrow \langle E'_T \rangle$ are not appropriate for the incremental conversion of collision energy $\langle \Delta E_T \rangle \rightarrow \langle \Delta E'_T \rangle$.[35] The DIPR-DIP calculations actually favour conversion into vibration, $\langle \Delta E_T \rangle \rightarrow \langle \Delta E'_v \rangle$,[21] contrary to experimental observation.

## Conclusion

Measurements of vibrational energy disposal among the products of thermal, and superthermal collisions of $Xe(^3P_2)$ with hydrogen halides and with methyl iodide have emphasised the close parallels between their reaction dynamics and those of the corresponding alkali-metal reactions. At the same time comparisons with the corresponding alkaline-earth-metal systems have also highlighted the distinctions that are introduced by changing the character of the potential-energy surface while still retaining the very strong kinematic constraints. In the accompanying paper, attention is turned to the question of angular momentum disposal and the consequences of a simple vectorial model (the constant orbital angular momentum model which parallels the scalar CPR model) are explored.

We are grateful to the S.E.R.C. for the award of a research studentship (to W. S. H.), to Professor A. G. Ureña (Complutense University, Madrid) for very helpful discussions, and to a referee for helpful comments related to the CPR approximations.

## References

1 D. R. Herschbach, *Adv. Chem. Phys.*, 1966, **10**, 233.
2 C. Noda, J. S. McKillop, M. A. Johnson, J. R. Waldeck and R. N. Zare, *J. Chem. Phys.*, 1986, **85**, 856.
3 D. S. Y. Hsu, N. D. Weinstein and D. R. Herschbach, *Mol. Phys.*, 1975, **29**, 257.
4 D. A. Case and D. R. Herschbach, *Mol. Phys.*, 1975, **30**, 1537.
5 D. S. Y. Hsu, G. M. McClelland and D. R. Herschbach, *J. Chem. Phys.*, 1974, **61**, 4927.
6 K. M. Johnson, J. P. Simons, P. A. Smith, C. Washington and A. Kvaran, *Mol. Phys.*, 1986, **57**, 255.
7 M. S. de Vries, G. W. Tyndall, C. L. Cobb and R. M. Martin, *J. Chem. Phys.*, 1986, **84**, 3753.
8 R. J. Hennessy and J. P. Simons, *Mol. Phys.*, 1981, **77**, 1027.
9 G. M. McClelland and D. R. Herschbach, *J. Phys. Chem.*, 1987, **91**, 2698.
10 C. Noda and R. N. Zare, *J. Chem. Phys.*, 1987, **86**, 3968.
11 A. Siegel and A. Schultz, *J. Chem. Phys.*, 1982, **76**, 4513.
12 A. Siegel and A. Schultz, *J. Chem. Phys.*, 1980, **72**, 6227.
13 A. Gupta, D. S. Perry and R. N. Zare, *J. Chem. Phys.*, 1980, **72**, 6327.
14 T. Munakata, Y. Matsumi and T. Kasuya, *J. Chem. Phys.*, 1983, **79**, 1698.
15 P. Chevrier, B. Collings, P. Das, J. C. Polanyi, M. G. Prisant and J. P. Visticot, *Chem. Phys.*, 1989, **133**, 1.
16 H. W. Cruse, P. J. Dagdigian and R. N. Zare, *Faraday Discuss. Chem. Soc.*, 1973, **55**, 277.
17 See data listed by B. E. Holmes and D. W. Setser, in *Physical Chemistry of Fast Reactions*, ed. I. W. M. Smith (Plenum Press, New York, 1980).
18 P. B. Moon, C. T. Rettner and J. P. Simons, *J. Chem. Soc., Faraday Trans. 2*, 1978, **74**, 630.
19 J. P. Simons and C. Washington, *J. Phys. E*, 1984, **17**, 581.
20 R. J. Donovan, P. Greenhill, M. A. MacDonald, A. J. Yencha, W. S. Hartee, K. Johnson, C. Jouvet, A. Kvaran and J. P. Simons, *Faraday Discuss. Chem. Soc.*, 1987, **84**, 221.
21 W. S. Hartee, *Ph.D Thesis* (University of Nottingham, 1988).
22 K. Johnson, A. Kvaran and J. P. Simons, *Mol. Phys.*, 1983, **50**, 981.
23 K. Johnson, R. Pease, J. P. Simons, P. A. Smith and A. Kvaran, *J. Chem. Soc., Faraday Trans. 2*, 1986, **82**, 1281.
24 W. Demtroder, *Laser Spectroscopy* (Springer-Verlag, Berlin, 1981).
25 P. J. Hay and T. H. Dunning, *J. Chem. Phys.*, 1977, **66**, 1306; 1978, **69**, 2209.
26 K. Tamagake, D. W. Setser and J. H. Kolts, *J. Chem. Phys.*, 1981, **74**, 4286.
27 A. M. G. Ding, L. J. Kirsch, D. S. Perry, J. C. Polanyi and J. L. Schreiber, *Faraday Discuss. Chem. Soc.*, 1973, **55**, 252.
28 M. Shapiro and Y. T. Zeiri, *J. Chem. Phys.*, 1979, **70**, 5264.
29 R. S. F. Chang, *J. Chem. Phys.*, 1982, **76**, 2943.
30 R. B. Berntein and B. E. Wilcomb, *J. Chem. Phys.*, 1977, **67**, 5809.
31 G. Rotzoll, R. Viard and K. Schugerl, *Chem. Phys. Lett.*, 1975, **35**, 353.
32 P. J. Kuntz, M. Mok and J. C. Polanyi, *J. Chem. Phys.*, 1969, **50**, 1623.
33 D. R. Herschbach, *Faraday Discuss. Chem. Soc.*, 1973, **55**, 233.
34 M. G. Prisant, C. T. Rettner and R. N. Zare, *J. Chem. Phys.*, 1984, **81**, 2699.
35 P. J. Kuntz, *Mol. Phys.*, 1972, **23**, 1035.

*Paper* 9/03435H; *Received* 10*th August*, 1989